

The Emergence of the Thick Disk in a CDM Universe II: Colors and Abundance Patterns.

Chris B. Brook,¹ Brad K. Gibson,^{2,3} Hugo Martel,¹ & Daisuke Kawata²

ABSTRACT

The recently emerging conviction that thick disks are prevalent in disk galaxies, and their seemingly ubiquitous old ages, means that the formation of the thick disk, perhaps more than any other component, holds the key to unravelling the evolution of the Milky Way, and indeed all disk galaxies. In Paper I, we proposed that the thick disk was formed in an epoch of gas rich mergers, at high redshift. This hypothesis was based on comparing N-body/SPH simulations to a variety of Galactic and extragalactic observations, including stellar kinematics, ages and chemical properties. Here we examine our thick disk formation scenario in light of the most recent observations of extragalactic thick disks. In agreement, our simulated thick disks are old and relatively metal rich, with V-I colors that do not vary significantly with distance from the plane. Further, we show that our proposal results in an enhancement of α -elements in thick disk stars as compared with thin disk stars, consistent with observations of the relevant populations of the Milky Way. We also find that our scenario naturally leads to the formation of an old metal weak stellar halo population with high α -element abundances.

Subject headings: galaxies: evolution — galaxies: formation — galaxies: halos — galaxies: structure — numerical methods

1. INTRODUCTION

The emerging conviction that thick disks are prevalent in disk galaxies offers rich possibilities of new insights into the origin and evolution of such galaxies. Using the current thick disk as a fossil record, holding details of the processes occurring at early stages of galaxy formation has become one of the keys to shedding light on the origin of disk galaxies. The thick disk of the Milky Way was discovered over twenty years ago (Bernstein 1979; Gilmore & Reid 1983). Relative to

¹Département de physique, de génie physique et d'optique, Université Laval, Québec, QC, Canada G1K 7P4

²Centre for Astrophysics & Supercomputing, Swinburne University, Hawthorn, Victoria, 3122, Australia

³School of Mathematical Sciences, Monash University, Clayton, Victoria, 3800, Australia

the thin disk, thick disk stars are kinematically warm, and lag in rotation by $\sim 20 - 40 \text{ km s}^{-1}$ (Chiba & Beers 2000). Studies have consistently found thick disk stars are old, almost exclusively older than 10 Gyrs (e.g. Gilmore & Wyse 1985; Edvardsson et al. 1993; Fuhmann 1998; Girard & Soubrian 2004). Yet thick disk stars are relatively metal rich, with the peak of the metallicity distribution of thick disk stars at $[\text{Fe}/\text{H}] \sim -0.6$ (e.g. Chiba & Beers 2000). Thick and thin disk stars are chemically well separated (e.g. Fuhmann 1998; Prochaska et al. 2000; Tautvaišienė et al 2001; Feltzing, Bensby, & Lundström 2003; Mashonkina et al. 2003; Reddy et al. 2003; Schröder & Pagel 2003; Girard & Soubrian 2004; Bensby et al. 2005, hereafter BFLI), with thick disk stars having notably higher α -elements, with a ratio of α/Fe for given Fe content systematically higher than thin disk stars. There is at most only a very weak gradient in metallicity with height above the plane in the thick disk (Gilmore, Wyse, & Jones 1995; Rong, Buser, & Karali 2001), in fact BFLI found that abundance trends appear to be invariant with vertical height.

Thick disks have now been shown to be prevalent in disk galaxies (Dalcanton & Bernstein 2002, hereafter DB02). Surface photometry of a sample of 47 edge-on disk galaxies in DB02 also showed that extragalactic thick disks are red. The next step in studying extragalactic thick disks was recently taken by Mould (2005, hereafter M05), who resolved the stellar population of a nearby sample of edge-on disk galaxies, to reveal the properties as a function of height above the plane. All four galaxies of the M05 sample have thick disks composed of red stellar populations. The gradient of color with height, $\Delta(V - I)/\Delta Z$ is almost zero, or slightly positive. From the color magnitude diagram (CMD) analysis, M05 concludes that the thick disks consist of old and relatively metal rich populations, and their stellar population is independent of height. A study of the stellar content of NGC 55 by Davidge (2005, hereafter D05) similarly finds that stars associated with the thick disk are old (ages ~ 10 Gyrs), with the majority being in the metallicity range $-1.2 < [\text{Fe}/\text{H}] < -0.7$. A further recent study by Tikhonov, Galazutdinova & Drozovsky (2005) also find evidence for thick disks in the three nearby spiral galaxies for which they analyse AGB and RGB stars. The results of M05, D05 and Tikhonov, Galazutdinova & Drozovsky (2005) are consistent with the conclusions of DB02, as well as with observations of the Milky Way thick disk.

A disk galaxy simulated (hereafter, simulated galaxies will be referred to as sGALS to avoid confusion with real galaxies) using our chemodynamical galaxy formation code, GCD+, was shown to have a thick disk component (Brook et al. 2004b, hereafter BKGF). This was evidenced by the velocity dispersion versus age relation for stars around solar radii, which showed an abrupt increase in velocity dispersion at lookback time of ~ 8 Gyrs, in excellent agreement with observation. By examining and comparing these simulations with observations, we proposed that thick disks form from gas which is accreted during a chaotic period of hierarchical clustering of gas rich "building blocks" at high redshift (BKGF). This formation scenario was shown to be consistent with observations of both the Galactic and extragalactic thick disks.

In this study, we examine four disk sGALS, and compare their thick disk stellar populations to recent observations of extragalactic thick disks, paying particular attention to the observations in M05. Age and metallicity gradients with height above the plane, as well as integrated V-I colors are derived. Comparison is also made with the studies of extragalactic thick disks in DB02 and D05. Further, we examine the abundance ratio of α -elements with respect to iron in the stellar populations of the thin and thick disks, as well as halos of our sGALS. These will provide further important tests of our thick disk formation scenario, and tie in to current studies on the formation of the stellar halo component of disk galaxies.

2. THE CODE AND MODELS

Our simulated galaxies (sGALS) are formed using our galactic chemodynamical evolution code, GCD+. This N-body/smoothed particle hydrodynamics (SPH) code self-consistently follows the effects of gravity, gas dynamics, radiative cooling, and star formation. GCD+ also takes into account metal enrichment and energy released by both Type II (SNe II) and Type Ia (SNe Ia) supernovae, as well as the metal enrichment from intermediate mass stars. Full details of GCD+ can be found in Kawata & Gibson (2003). We apply the *Adiabatic Feedback Model* described in Brook et al. (2004a). The model assumes that the gas within the SPH smoothing kernel of SNe II explosions is in adiabatic phase, in a fashion similar to a model presented in Thacker & Couchman (2000). This allows us to form late-type sGALS which each have a dominant disk component, and a less massive, relatively metal poor halo component (Brook et al. 2004a).

We employ here a semi-cosmological version of GCD+ based upon the galaxy formation model of Katz & Gunn (1991). The initial condition is an isolated sphere which consists of dark matter and gas and whose total mass is M_{tot} . This top-hat overdensity has an amplitude, δ_i , at initial redshift, z_i , which is approximately related to the collapse redshift, z_c , by

$$z_c = 0.36\delta_i(1 + z_i) - 1 \quad (1)$$

(e.g. Padmanabhan 1993). Small scale density fluctuations are superimposed on each sphere, parameterized by σ_8 . These perturbations are the seeds for local collapse and subsequent star formation. To incorporate the effects of longer wavelength fluctuations, a solid-body rotation corresponding to a spin parameter, λ , is imparted to the initial sphere.

We assume an Einstein de-Sitter CDM model with $\Omega_0 = 1$, $\lambda_0 = 0$, $H_0 = 50 \text{ km s}^{-1} \text{ Mpc}^{-1}$, baryon fraction, $\Omega_b = 0.1$, and $\sigma_8 = 0.5$. (but see § 4 below). We also assume a star formation efficiency $c_* = 0.05$ (Kawata & Gibson 2003). We run four models of sGALS (sGAL1-4), changing arbitrarily the parameters of z_c , M_{tot} and λ . The parameter values adopted are summarized in Table 1. Values for z_c are all well within the range of distributions for formation times

of Milky Way sized dark matter halos expected in a concordance Λ CDM cosmology (e.g. Power 2003). Along with these variations in parameters, different random seeds for initial density perturbations are incorporated in the initial conditions of each sGAL, creating evolutionary diversity in our sample. The random seeds are deliberately chosen to ensure no major merger occurs in late epochs ($z < 1$). These initial conditions, with large values of λ , lead to morphology of late-type disk galaxies for all four sGALS. We employed 38911 dark matter and 38911 gas/star particles for each model, making the resolution comparable to other recent studies of disk galaxy formation.

3. RESULTS

3.1. Vertical Stellar Population Gradient for Thick Disk Stars

Figure 1 shows I -band images of each sGAL at the present, displayed both face-on (X-Y plane, where the disk rotation axis is set to be Z-axis) and edge-on (X-Z plane, lower panels). The four sGALS are reasonably uniform in their morphology, although sGAL4 at first glance appears to have a more prominent bulge than the other three. Each has a dominant young, metal rich thin disk. The stellar halo components are old and metal poor. The surface density profiles of disk component for all four sGALS are reasonably well fitted by exponentials.

Evidence that our four sGALS have thick disk components is provided by the velocity dispersion-age relation. Figure 2 shows the velocity dispersion in the direction perpendicular to the disk plane (Z direction) as a function of age for stars in the “solar neighborhood” of our four sGALS. The solar neighborhood in sGALS is defined as an annulus bounded by $6 < R_{XY} < 10$ kpc, and $|Z| < 1$ kpc, where R_{XY} is the radius in the disk plane. The observed velocity dispersion-age relation for solar neighborhood stars are also shown as triangles with error bars, as read from Figure 3 of Quillen & Garnett (2001), who use the data of Edvardsson et al. (1993). The observed velocity dispersion

Table 1. Model Parameters and the age range, t_{thick} , for the definition of thick disk stars in our study.

Galaxy	z_c	$M_{\text{tot}}(M_{\odot})$	λ	t_{thick}
sGAL1	1.8	5×10^{11}	0.0675	10.0-8.5
sGAL2	1.9	5×10^{11}	0.0675	10.4-8.5
sGAL3	2.0	1×10^{12}	0.0600	11.4-9.0
sGAL4	2.2	5×10^{11}	0.0675	11.0-9.0

is relatively constant for the past ~ 9 Gyrs¹, but shows an abrupt increase at ~ 10 Gyrs ago. The older stars with high velocity dispersion are recognized as thick disk stars. The velocity dispersion for the four sGALS show qualitatively very similar behavior, with plateaus interrupted by abrupt increases of velocity dispersion, at lookback times of between 8 and 10 Gyrs. The implication is that each of our sGALS also has an old thick disk component. In sGAL1 and sGAL2, these abrupt increases are more recent, at ~ 8 Gyrs ago, compared with sGAL3 and sGAL4, whose jump in velocity dispersion occurred closer to 10 Gyrs ago. The differences in the lookback time of these increases in velocity dispersion in our sGALS is partly related to the differences in collapse redshift, z_c , in our initial conditions.

We use the timing of these increases in velocity dispersion of our sGALS as a pointer to the thick disk formation era of each simulation. In Figures 3-6, we plot four snapshots at different time-steps in the evolution of our sGALS during these thick disk formation epochs. In each sGAL, these epochs are defined by multiple mergers of gas rich galactic building blocks. The first panel in each plot shows a number of "building blocks", and it is clear that these are gas rich. As is detailed in BKGF, we confirmed that the gas mass to stellar mass ratio within these building blocks is high at this epoch. A turbulent period of mergers then ensues. At this time, gas which carries significant angular momentum ends up a disk structure. However, the gaseous disk is kinematically heated up by these perturbations of merging building-blocks, and has high-velocity dispersion. Consequently the stars born in the disk at this period have high-velocity dispersion, and are subsequently identified as thick disk stars.

This epoch is also characterized by rapid star formation. Global star formation rate (SFR) as a function of lookback time for the sGALS is plotted in Figure 7. The thick disk formation epoch shown in Figures 3-6 corresponds closely to the peak of SFR. The peak of SFR for sGAL1 and sGAL2 is later than that for sGAL3 and sGAL4, corresponding to the earlier thick disk formation epoch in sGAL3 and sGAL4, as reflected in Figure 2 and Figures 3-6. By the end of the thick disk formation epoch, the thin disk component starts to be built up (see BKGF for more details).

Following BKGF, we identify disk stars which form in this epoch as thick disk stars. Thus, we refer to disk star particles forming in the period highlighted in Figures 3-6 as thick disk stars. The age range for the definition of the thick disk is summarized in Table 1. We arbitrarily decided this age range, based on velocity dispersion (Fig. 2), snapshots (Figs. 3-6), and star formation rates (Fig. 7). We confirmed that the results shown in this paper are not sensitive to modest changes in these age definitions. An additional criterion, applied to extract disk stars, is a rotational velocity of greater than 50km s^{-1} , which eradicates halo stars which form in the period that the thick disk

¹The more recent study by Nordström et al. (2004) finds that *thin* disk stars do show an increase of velocity dispersion with age, but this does not impact the analysis here.

is built up.

We confirm that the properties of the thick disk stars identified are similar to those observed in the thick disk of the Milky Way (see BKGF for more details). The rotation velocity of thick disk lags that of thin disk stars by $20 - 30 \text{ km s}^{-1}$. We derive thick disk scale-heights of 1.3, 1.4, 1.1, and 1.4 kpc for sGAL1-4 respectively, compared to the thin disk scale-heights of 0.52, 0.55, 0.6 and 0.45 kpc. The thick disk stars are uniformly old, as expected by its definition. We will demonstrate below that the thick stars in sGALS also have characteristic metallicities observed in the Milky Way and external disk galaxies.

The key questions of the current study of sGALS are the variation in the metallicities, age, and hence colors of thick disk stars as a function of the distance from the disk plane, i.e. height ($|Z|$), as well as how their abundance ratios differ from later forming thin disk stars. Figure 8 displays the mean iron abundance, which we call metallicity hereafter, of thick disk stars, as a function of $|Z|$. Thick disk stars of sGAL1, sGAL2 and sGAL4 have metallicities in the range of $\langle [\text{Fe}/\text{H}] \rangle$ between -0.5 and -0.6 , closely resembling the thick disk of the Milky Way, while thick disk stars of sGAL3 have a significantly lower metallicity, $\langle [\text{Fe}/\text{H}] \rangle \sim -0.8$. This may be related to the fact that the thick disk of sGAL4 is significantly less massive than the other sGALS. However, to examine this, we need a statistically significant sample, and thus we are now trying to increase the number of sGALS (Renda et al. 2005). The important thing is that very little gradient is present in Figure 8 for the thick disk star particles of any sGAL.

Figure 9 demonstrates the age of the thick disk star particles against $|Z|$. Little trend of age with height can be said to exist. This is not trivial, because the age range for the definition of the age of the thick disk is wide enough to have more significant age gradient. It looks a little odd that sGAL4 thick disk stars are older on average than those of sGAL3, seemingly contrary to the time of the epoch given in Table 1. This is due to the sharper downturn in SFR in sGAL4, as seen in Figure 7, which means that a larger fraction of thick disk stars in sGAL4 were born at the early time of the thick disk formation epoch, compared with sGAL3.

As a result of a lack of significant gradient in neither age nor metallicity with height, the thick disk star particles have no real color gradient. Figure 10 shows the mean $V - I$ color as a function of $|Z|$. Here we derive the mean $V - I$ color for the giant branch stars (RGB/AGB) of thick disk populations of the sGALS. Padova isochrones (Girardi et al. 2000) are used to derive the colors. We obtain the isochrone of the average age and metallicities seen in Figures 8 and 9 with linear interpolations are taken between the ages and metallicities provided by the Padova tables. Then the $V - I$ colors are derived by taking the initial mass function (IMF) weighted mean of the isochrone within the range of $-2.7 < I < -9.7$, which corresponds to the luminosity range applied in M05. The red colors of the giant branch stars reflects the age and metallicity of the thick disk populations, and there is no color gradient. These results are in good agreement with the colors, and lack of

color gradient, as observed in M05.

Figure 11 shows the $B - R$ and $R - K$, colors of our thick disk stars. Here the colors are derived from the integration of the luminosity of all thick disk stars which are still alive at the end of the simulations (redshift zero). Again, Padova isochrones are used to derive the colors. We see that these colors are relatively constant with height, at $B - R \sim 1.4 - 1.5$, and $R - K \sim 1.9 - 2.2$. These colors allow direct comparison with Figures 3 and 6 of DB02. Away from the plane, DB02 find a relatively narrow range of colors, with $B - R \sim 1.0-1.4$ and $R - K \sim 2.0 - 2.6$. In this study we do not examine sGALS with the same mass range as the 47 galaxies studied in DB02, but rather examine only L_* sGALS. Nevertheless, thick disks of the sGALS have colors which can explain the stellar populations observed in DB02 to envelope edge-on disk galaxies, which they interpret as thick disk components.

3.2. $[\alpha/\text{Fe}]$ vs. $[\text{Fe}/\text{H}]$ for Thin and Thick Disk and Halo Stars.

We next compare the abundance ratios of α -elements with respect to iron for different sGAL components, thin disk, thick disk and stellar halo. In order to best compare with observations, we look at star particles within the “solar neighborhood”, as defined above. Thin disk stars are defined as stars younger than 7 Gyr and rotating faster than 50km s^{-1} . The halo stars are represented by retrograde stars which formed before the end of the thick disk formation epoch as defined in Table 1. Note that the stars which have already formed in the building blocks which subsequently merge during thick disk formation have a strong tendency toward ending up in the halo (see Brook et al. 2004a)². The α -element abundances of the three components are plotted in Figures 12-15. Abundances of Oxygen and Magnesium are used to define our α -elements. The spread of the distributions in the $[\text{Fe}/\text{H}]$ axis is taken to include approximately 90% of stars within each component.

It is evident that in all four sGALS, thick disk stars have higher α -element abundances than thin disk stars, even where they overlap in metallicity, $[\text{Fe}/\text{H}]$. These thick disk abundances are characteristic of dominant enrichment from SNe II. These results match very nicely with recent observations, (e.g. Fuhmann 1998; Prochaska et al. 2000; Tautvaišienė et al 2001; Feltzing, Bensby, & Lundström 2003; Mashonkina et al. 2003; Reddy et al. 2003; Schröder & Pagel 2003; Girard & Soubrian 2004; BFLI). Uncertainty in our models must be noted here, regarding star formation

²The tendency for accreted stars to be circularized and hence end up as part of the disk components, as highlighted by e.g. Meza et al. (2005), will only occur for stars accreted after a disk has already formed. The fraction is expected to be low in the Milky Way, because such stars are expected to have low metallicity, and the metallicity distribution function of solar neighbor stars suggests little population of such metal poor stars.

prescriptions, nucleosynthesis yields, and particularly SNe Ia time-scales, which are still little understood theoretically. It is, however, very encouraging that the overall trends of the difference in abundance patterns between thin and thick disk in the Milky Way can be reproduced with our thick disk formation scenario.

Halo stars in our sGALS also have high α -element abundances. As shown in Brook et al. (2004a), stars in the gas rich building blocks will preferentially accrete to the halo. Those formed in building blocks accreted at high redshift will have been enriched primarily by SNe II. Halo stars tend to have slightly higher $[\alpha/\text{Fe}]$ than thick disk stars. This seems to be because SNe II yields from higher mass stars have higher $[\alpha/\text{Fe}]$ (Woosley & Weaver 1995). The thin disk stars, which form in the later, more quiescent period in the evolution of our sGALS, are clearly formed from material more enriched by SNe Ia, which produces iron, and have lower $[\alpha/\text{Fe}]$.

4. DEPENDENCE ON THE COSMOLOGICAL MODEL

In this section, we address two potential limitations of our simulations: First, the fact that we assumed an Einstein de-Sitter model instead of the preferred “concordance model,” and second, the fact that our simulations deal with the collapse of an isolated top hat perturbation.

4.1. The Cosmological Model

In our simulations, the background cosmological model was an Einstein-de Sitter model with $\Omega_0 = 1$, $\lambda_0 = 0$, and $H_0 = 50 \text{ km s}^{-1} \text{ Mpc}^{-1}$. However, observations now favor a flat, cosmological constant model (Λ CDM) with $\Omega_0 = 0.27$, $\lambda_0 = 0.73$, and $H_0 = 71 \text{ km s}^{-1} \text{ Mpc}^{-1}$ (Bennett et al. 2003). While using a different model would have a major effect on simulations of large-scale structure formation from Gaussian random noise initial conditions, we can show that, in the context of the galaxy formation model we are using, the effect is negligible.

The cosmological parameters at redshift z can be expressed in terms of their present values using

$$\Omega(z) = \frac{\Omega_0(1+z)^3}{(1-\lambda_0+\Omega_0z)(1+z)^2+\lambda_0}, \quad (2)$$

$$\lambda(z) = \frac{\lambda_0}{(1-\lambda_0+\Omega_0z)(1+z)^2+\lambda_0} \quad (3)$$

(e.g. Martel & Wasserman 1990). Using the “concordance” values $\Omega_0 = 0.27$, $\lambda_0 = 0.73$, we find $\Omega = 0.99996$, $\lambda = 0.00004$ at the initial redshift $z_i = 40$. At redshift $z = 3$, by which time our

simulations have “turned around” we have $\Omega = 0.959$, $\lambda = 0.041$. Afterward, the system becomes significantly denser than the background universe and the cosmology becomes irrelevant. Even as late as $z_c = 1.8$, the smallest collapse redshift from our initial conditions, we have $\Omega = 0.886$, $\lambda = 0.114$. Hence, the model is very close to an Einstein-de Sitter model from the initial redshift up to the redshift of collapse. In particular, once the galaxies have formed, the repulsive force caused by the cosmological constant is totally negligible.

We still need to compare the evolutionary timescales, which are determined by the Hubble constant H_0 . The mean background density is given by $\bar{\rho} = \bar{\rho}_0(1+z)^3$. Using $\bar{\rho} \propto \Omega H^2$, we get $H = H_0(\Omega_0/\Omega)^{1/2}(1+z)^{3/2}$. We eliminate Ω_0/Ω using equation (2), and get

$$H(z) = H_0 [(1 - \lambda_0 + \Omega_0 z)(1+z)^2 + \lambda_0]^{1/2}. \quad (4)$$

This gives us the time-evolution of the Hubble parameter. Using this equation, we evaluate H at the collapse redshifts, using both the Einstein de-Sitter model and the concordance Λ CDM model. The results are listed in Table 2. The values of H at these redshifts are lower for the Λ CDM model, even though the present value H_0 for that model is larger.

Consider first the redshift interval $[z_i, z_c]$. As we argued above, the Λ CDM model is very close to the Einstein-de Sitter model in that range (that is, $\Omega \approx 1$, $\lambda \approx 0$). However, the Hubble parameter has a different value, and this implies a different evolution timescale. In the redshift range $[z_i, z_c]$, our Einstein-de Sitter model is *equivalent* to a Λ CDM model in which the system would evolve too fast because of the different Hubble parameter. This turns out to have no actual consequence. The relationship between initial and collapse redshift (eq. [1]) does not depend on any timescale. The collapse redshift is entirely determined by the dimensionless parameters z_i and δ_i . In our simulations, the background universe evolves faster than in the Λ CDM model (by about 30%), but the top hat perturbation itself also evolves faster, such that the collapse redshift will be the same in both models.

Consider now the interval $[z_c, 0]$ between the collapse redshift and the present. In this redshift interval, the system is essentially isolated and the cosmology is irrelevant. All we need to do is to

Table 2. Hubble parameter at collapse redshift (in units of $\text{km s}^{-1}\text{Mpc}^{-1}$)

Galaxy	z_c	$H(z_c, \text{EdS})$	$H(z_c, \Lambda\text{CDM})$
sGAL1	1.8	234	183
sGAL2	1.9	247	192
sGAL3	2.0	260	201
sGAL4	2.2	286	220

compare the elapsed time between $z = z_c$ and $z = 0$ to check that the simulations terminated at a time that truly corresponds to the present. For flat cosmological models ($\Omega_0 + \lambda_0 = 1$), the age of the universe at redshift z is given by

$$t = \frac{2}{3\lambda_0^{1/2}H_0} \arg \sinh \left[\left(\frac{\lambda_0}{\Omega_0} \right)^{1/2} (1+z)^{-3/2} \right]. \quad (5)$$

Using this formula, we can compute the lookback time $t(0) - t(z)$ at $z = z_c$ for our four simulated galaxies. The results are shown in Table 3. The differences between the two models is only of order 2 – 3%, which is negligible.

Hence, we conclude that having considered an Einstein de-Sitter model instead of the concordance Λ CDM model does not invalidate our simulations.

4.2. Merger Histories

The semi-cosmological model used in this study offers the advantage of allowing several galaxies, which include detailed chemical enrichment histories, to be studied within a hierarchical context. Here we do a larger survey of the merger history of halos using N-body simulations in a fully cosmological concordance model. This will allow us to examine further the merging aspects of our proposed thick disk formation scenario with greater statistics in a less idealized cosmological context.

We perform N-body simulations of structure formation in a Λ CDM model with $\Omega_0 = 0.27$, $\lambda_0 = 0.73$, and $H_0 = 71 \text{ km s}^{-1} \text{ Mpc}^{-1}$, using a P³M algorithm (Efstathiou et al. 1985; Martel 1991). In our initial run, we simulated a comoving cubic volume of size $L_{\text{box}} = 100 \text{ Mpc}$, using 128^3 particles. The mass per particle was $1.801 \times 10^{10} M_\odot$. In this simulation, we identified a region of size $30 \text{ Mpc} \times 35 \text{ Mpc} \times 28 \text{ Mpc}$ in which several Milky-Way-like halos formed, and we zoom-in by increasing the resolution of the code by 2 in each direction in the region of interest

Table 3. Lookback times (in units of Gyrs)

Galaxy	z_c	lookback time (EdS)	lookback time (Λ CDM)
sGAL1	1.8	10.25	9.97
sGAL2	1.9	10.40	10.16
sGAL3	2.0	10.53	10.28
sGAL4	2.2	10.76	10.62

and rerunning the simulation. The simulation with zoom-in has a total of 2.5 million particles, and the mass per particle in the region of interest is $2.251 \times 10^9 M_\odot$. This is sufficient to resolve the relatively large building blocks which we are interested in, in this study. We found in the region of interest 58 halos with masses in the range $(0.5 - 1.1) \times 10^{12} M_\odot$.

We have computed the merger trees for all 58 halos which are Milky Way analogs. Two trees are shown in Figure 16. On each panel, the area of the circles are proportional to the mass of the halos, and time increases from top to bottom. The black circle identifies a particular halo that formed by a “major” merger or a series of “significant” mergers. Halo 1 formed by the merger of 5 halos of comparable masses occurs between 9.3 and 7.7 Gyrs ago (resembling sGAL1). For halo 2, several mergers take place between 11.0 and 10.3 Gyrs ago (and may be compared with sGAL3); this involves 4 halos of significant mass. Another merger occurs between 9.3 and 7.7 Gyrs ago, and a smaller one between 7.7 and 5.0 Gyrs ago. In this study, we are interested in merger events which are not necessarily “major mergers”, in which halos of comparable mass are involved, but rather mergers which we may call “significant”, in that they add a significant amount of mass to the forming central halo. In order to quantify this, we define “significant” in this section as a “building block” with mass $\geq 10^{10} M_\odot$ which adds at least 4% to the mass of the forming halo. Such a merger event is able to disturb the disk structure which is forming (Quinn, Hernquist, & Fullagar 1993). We plot the average number of such “building blocks” versus lookback time in Figure 17. In order to qualify, the “building block” must be merged to the central halo³ by the next time interval, so that Figure 17 summarizes the merger history of the final halo. The number of “building blocks” at each time interval includes the central halo, so a value of one on the Y-axis corresponds to there being only a central galaxy. We see that, on average, halos of mass comparable to the Milky Way only have a few “significant” mergers, and that most occur between ~ 8 and ~ 11 Gyrs ago. We include all 58 final halos of mass $(0.5 - 1.1) \times 10^{12} M_\odot$ in this plot. Several, (~ 15), halos have major mergers at late epochs (less than 5 Gyrs ago), and are thus probably not good candidates for hosting late type galaxies. Omitting these galaxies from our study would extenuate our findings in this section that the bulk of the “significant” merging events of Milky Way type dark halos occur at high redshift.

5. DISCUSSION

Several scenarios have been put forward to explain the origin of the thick disk of the Milky Way, which has become established as a separate component from the thin disk. A review of these was made in BKGF and will not be repeated here. Readers are also referred to reviews by Gilmore,

³or largest halo; at early times there are often several similar sized halos, like in halo 1 of Figure 16

Wyse, & Kuijken (1989) and Wyse (2004). The importance of thick disk formation has seemingly been enhanced by recent observations suggesting that thick disks are prevalent in spiral galaxies, with their seemingly ubiquitous old age implying that their formation may be a key in unraveling the formation of such galaxies. In BKGF, we proposed a scenario in which the bulk of thick disk stars forms in a period of multiple merging of gas-rich building blocks at high redshift, prior to thin disk stars forming. As this is very much a follow up paper to BKGF, we will not repeat our analysis of the various thick disk scenarios, and their consistency with current observations. Suffice to say that we believe our scenario to be consistent with both Galactic and extragalactic observations. In this paper we have analyzed our thick disk formation scenario in light of new results in M05, as well as explicitly examining α -element abundance signatures.

By resolving individual stars in four local edge-on disk galaxies with the *Hubble Space Telescope*, M05 confirmed that a) thick disks are common features of spiral galaxies, b) thick disk stars are old, c) relatively metal rich and, d) have no significant vertical metallicity gradient. These observations do not support thick disks forming from shredded stars from accreting satellites (because they should be metal poor), or slow heating of the thin disk (a color gradient with height, and young thick disk stars would be expected). Lack of detection of a vertical metallicity gradient also puts a strong constraint on a scenario which involves *slow* dissipative collapse. We have shown in Figures 8 and 9 that our thick disk formation scenario is consistent with these observations. Especially, there is no vertical trend in the metallicity or age, and thus color. This is because in our thick disk formation scenario the thick disk forms from well-enriched gas disk in situ, in a relatively short period. Astaration during and after the mergers, as well as the ongoing dissipative infall of gas (see e.g. Murali et al. 2002) eliminates difference of metallicity of thick disk forming material, which leads to a relatively homogeneous metal rich and old stellar population, independent of vertical height. The M05 result is supported by other recent studies, D05 and Tikhonov, Galazutdinova & Drozovsky (2005).

Our thick disk stars have a combination of ages and metallicities which are able to explain the colors which DB02 find in the diffuse envelope components they observe in their sample of 47 edge-on disk galaxies, as shown in Figure 11. They believe that these envelopes are best explained by the prevalence of thick disks in spiral galaxies.

A study by Seth, Dalcanton, & de Jong (2005) of 6 nearby edge-on late type galaxies with resolved stellar populations also finds evidence for a thick disk or halo population, but their preliminary analysis of red giant branch colors indicate that this stellar envelope is more metal poor than those found by M05 and D05, with metallicities ranging between $-1.2 < [\text{Fe}/\text{H}] < -1.7$. This might suggest a diversity of the stellar population of the thick disks among different disk galaxies. Our four sGALS do not have such low metallicity. However, more statistical sample of sGALS with different masses and merger histories might explain such observations.

The building blocks which merge at high redshift in our thick disk formation scenario have primarily been enriched by SNe II. We have shown in Figures 12-15 that our thick disk formation scenario naturally explains the high α enhanced abundance pattern observed in thick disk stars compared to thin disk stars (e.g. Reddy et al. 2003; Girard & Soubrian 2004; BFLI). This is because in our scenario thick disk stars form earlier than thin-disk stars, which have more chance to be enriched more by SNe Ia. The other important fact affecting enhanced α -element abundances is high star formation rates during the merger epoch in which the thick disks form in our sGALS. Evidence that the thick disk has had a more intense star formation history than the thin disk was found by BFLI, and Mashonkina et al. (2003).

In order to simulate several sGALS with high resolution required for this study, use was made of simplified initial conditions. To place our study on a firmer cosmological background, we have used N-body simulations employing the concordance Λ CDM values to show that Milky Way sized dark halos evolve in a manner which supports our thick disk formation scenario. Most of the mass of such halos are accreted from the merging of a few intermediate sized ($> 10^{10}M_{\odot}$) building blocks, with a period of peak merging activity of such halos at lookback time of $\sim 8 - 11$ Gyrs. This is consistent with the study of Zentner & Bullock (2003), who find that dark halos of mass $\sim 1.4 \times 10^{12}M_{\odot}$ have a characteristic phase of mergers/disruption of subhalos of mass $\sim 1 - 10 \times 10^{10}M_{\odot}$ at a lookback time of ~ 10 Gyrs. In fact, Zentner & Bullock (2003) remark on the proximity in time of this merger phase with the ages of Milky Way and extragalactic thick disks. The timescale of our merger period is also consistent with distributions for formation times of Milky Way sized dark matter halos expected in high resolution simulations of concordance Λ CDM cosmology (e.g. Power 2003).

Our thick disk formation scenario is nicely coupled with the formation of an old, metal weak stellar halo population with α -element enhancement. In Brook et al. (2004a), accretion of stars to the halo in gas rich merger events was highlighted as necessary in creating low mass, low metallicity stellar halos in sGALS. Hence, many such halo stars formed in building blocks prior to the multiple merging epoch. The relatively low masses (recall the well established mass-metallicity relation for galaxies), and short times afforded for star formation prior to merging, ensure that these stars are metal poor. This can explain the oldest, and most metal poor halo stars. Figures 12-15 show that the halo stars will also have α -element enhancement. This halo star formation scenario was also highlighted in a recent semi-analytical study by Robertson et al. (2005), who showed that building blocks which merge at high redshift are likely to be a few relatively large ($\sim 5 \times 10^{10}$) dwarf irregular analogs, with α -element enhancement.

We feel it necessary to re-iterate the comment made in BKGf that late, direct accretion of stars after a disk has formed, in the manner described in Quinn, Hernquist, & Fullagar (1993) can also play a role in contributing to the thick disk population (e.g. Brook, Kawata, & Gibson 2003;

Yanny et al. 2003; Martin et al. 2004; Navarro, Helmi, & Freeman 2004; Meza et al. 2005). Such accretion has been shown to play a role in formation of the stellar halo (e.g. Ibata, Gilmore, & Irwin 1994; Helmi et al. 1999; Brook, Kawata, & Gibson 2003).

One recent study needs to be mentioned here. Yoachim & Dalcanton (2005) present evidence for the existence of a counter-rotating thick disk in FGC 227. Existence of counter-rotating thick disks would rule out models in which thick disks forms purely by monolithic collapse or from heating of a previous thin disk, and strongly favors accretion/merger models. The initial conditions of our models, in which a solid body rotation is imparted on our initial sphere, means that we cannot directly test for the existence of counter-rotating thick disks in the sGALS presented in this paper. All building blocks of significant mass which merge during thick disk formation epoch in our four sGALS have prograde rotation. However, it would not be surprising that in a multiple merger period there would be building blocks which have counter-rotation. Hence, our thick disk formation scenario remains a good candidate for explaining such observations. However, more statistical observations and simulations based on full-cosmological context are required to test our scenario.

Firsly we thank Jeremy Mould whose advanced provision of results, and insightful correspondence, provided the impetus for this study. We also thank Peter Yoachim and Julianne Dalcanton for providing results of their study on extragalactic thick disk ahead of publication. Simulations were performed on Swinburne University Supercomputer, those of the Australian Partnership for Advanced Computing, and on “Purplehaze,” the Supercomputer facility at Université Laval. CB and HM thank the Canada Research Chair program and NSERC for support. BKG and DK acknowledge the financial support of the Australian Research Council through its Discovery Project program.

REFERENCES

- Bennett, C. L. et al. 2003, *ApJS*, 148, 1
- Brook, C. B., Kawata, D., & Gibson, B. K. 2003, *ApJ*, 585, 125
- Brook, C. B., Kawata, D., Gibson, B. K., & Flynn C. 2004a, *MNRAS*, 349, 52
- Brook, C. B., Kawata, D., Gibson, B. K., & Freeman K. 2004b, *ApJ*, 612, 894 (BKGF)
- Bensby, T., Feltzing, S., Lundström, I., & Ilyin, I. 2005, *A&A*, in press (BFLI)
- Bernstein, D. 1979, *ApJ*, 234, 829

- Chiba, M., & Beers, T. C. 2000, *AJ*, 119, 2843
- Dalcanton, J. J., & Bernstein, R. A. 2002, *AJ*, 124, 1328 (DB02)
- Davidge, T. J. 2005, *ApJ*, in press (astro-ph/0501173) (D05)
- Edvardsson, B., Anderson, J., Gustafsson, B., Lambert, D. L., Nissen, P. E., & Tomkin, J. 1993, *A&A*, 275, 101
- Efstathiou, G., Davis, M., Frenk, C. S., & White, S. D. M. 1985, *ApJS*, 57, 241
- Feltzing, S., Bensby, T., & Lundström, I. 2003, *A&A*, 397, 1
- Furhmann, K. 1998, *A&A*, 338, 161
- Girard, P., & Soubrian, C. 2004, in *Three-dimensional Universe with Gaia*, 4-7 October 2004, Observatoire de Paris-Meudon, France (ESA SP-576), eds. M. Perryman & C. Turon
- Girardi, L., Bressen, A., Bertelli, G., & Chiosi, C. 2000, *Ap&SS*, 141, 371
- Gilmore, G., Wyse, R. F. G., & Kuijken, K. 1989, *ARA&A*, 27, 555
- Gilmore, G., Wyse, R. F. G., & Jones, J. B. 1995, *AJ*, 109, 3
- Gilmore, G., & Reid, N. 1983, *MNRAS*, 202, 1025
- Gilmore, G., & Wyse, R. F. G. 1985, *AJ*, 90, 2015
- Helmi, A., White, S. D. M., de Zeeuw, P. T., & Zhao, H. 1999, *Nature*, 402, 53
- Ibata, R. A., Gilmore, G., & Irwin, M. J. 1994, *Nature*, 370, 194
- Kawata, D., & Gibson, B. K. 2003, *MNRAS*, 340, 908
- Katz, N., & Gunn, J. E. 1991, *ApJ*, 377, 565
- Mashonkina, L., Gehren, T., Travaglio, C., & Borkova, T. 2003, *A&A*, 397, 275
- Martel, H., & Wasserman, I. 1990, *ApJ*, 348, 1
- Martel, H. 1991, *ApJ*, 366, 353
- Martin, N. F., Ibata, R. A., Ballazzini, M., Irwin, M. J., Lewis, G. F., & Dehnen, W. 2004, *MNRAS*, 348, 12
- Meza, A., Navarro, J. F., Abadi, G., & Steinmetz, M. 2005, *MNRAS*, in press.

- Mould, J. 2005, *AJ*, 129, 698
- Murali, C., Katz, N., Hernquist, L., Weinberg, D. H., & Davé, R. 2002, *ApJ*, 571, 1
- Navarro, J. F., Helmi, A., & Freeman, K. C. 2004, *ApJ*, 601, L43
- Nordström, B. et al. 2004, *A&A*, 418, 989
- Padmanabhan, T. 1993, *Structure Formation in the Universe* (Cambridge: Cambridge University Press)
- Power, C. 2003, Ph.D. Thesis, University of Durham
- Prochaska, J. X., Naumov, S. O., Carney, B. W., McWilliam, A., & Wolfe, A. M. 2000, *ApJ*, 120, 2513
- Quillen, A. C., & Garnett, D. 2001, in *Galaxy Disks and Disk Galaxies*, ASP Conference Series 203, eds. G. Jose, S. J. Funes, & E.M. Corsini (San Francisco: PASP), p. 87
- Quinn, P. J., Hernquist, L., & Fullagar, D. P. 1993, *ApJ*, 403, 74
- Reddy, B. E., Tomkin, J., Lambert, D. L., & Allende Prieto, C. 2003, *MNRAS*, 340, 304
- Renda, A., Gibson, B. K., & Kawata, D. 2005, in preparation
- Robertson, B., Bullock, J. S., Font, A. S., Johnston, K. S., & Hernquist, L. 2005, preprint (astro-ph/0501398)
- Rong, J., Buser, R., & Karali, S. 2001, *A&A*, 365, 431
- Schröder, K. P., & Pagel, B. E. J. 2003, *MNRAS*, 343, 1231
- Seth, A. C., Dalcanton, J. J., & de Jong, R. S. 2005, *AJ*, in press
- Tautvaišienė, G., Edvardsson, B., Tuominen, I., & Ilyin, I. 2001, *A&A*, 380, 578
- Thacker, R. J., & Couchman, H. M. P., 2000, *ApJ*, 545, 728
- Tikhonov, N. A., Galazutdinova, O. A., & Drozovsky, I. O. 2005, *A&A*, 431, 127
- Woosley, S. E., & Weaver, T. A. 1995, *ApJS*, 101, 181
- Wyse, R. F. G. 2004, in *The Local Group as an Astrophysical Laboratory*, ed. M. Livio (Cambridge: Cambridge University Press)
- Yanny, B. et al. 2003, *ApJ*, 588, 824

Yoachim, P., & Dalcanton, J. J. 2005, ApJ, in press

Zentner, A. R., & Bullock, J. S. 2003, ApJ, 598, 49

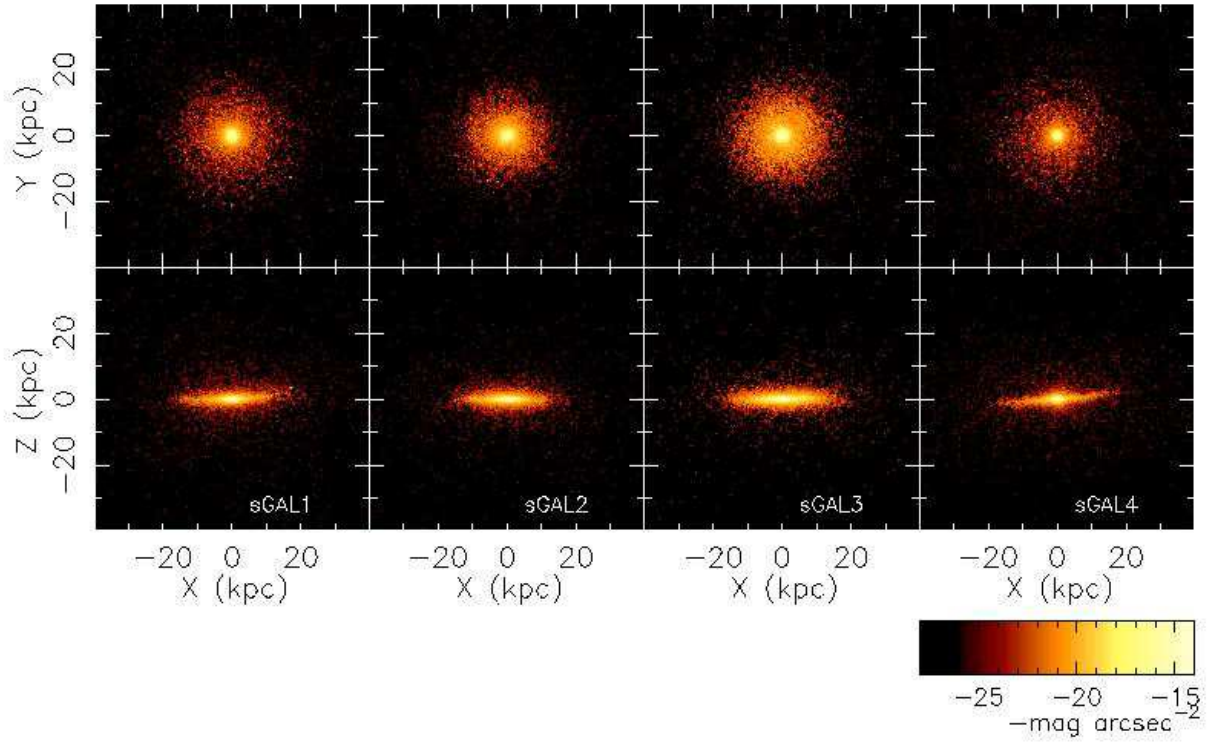


Fig. 1.— I-band image for our 4 sGALS at $z = 0$, shown in edge-on (X-Z plane, upper panels) and face-on (X-Y, lower) projections. The sGALS are dominated by young, metal rich thin disks.

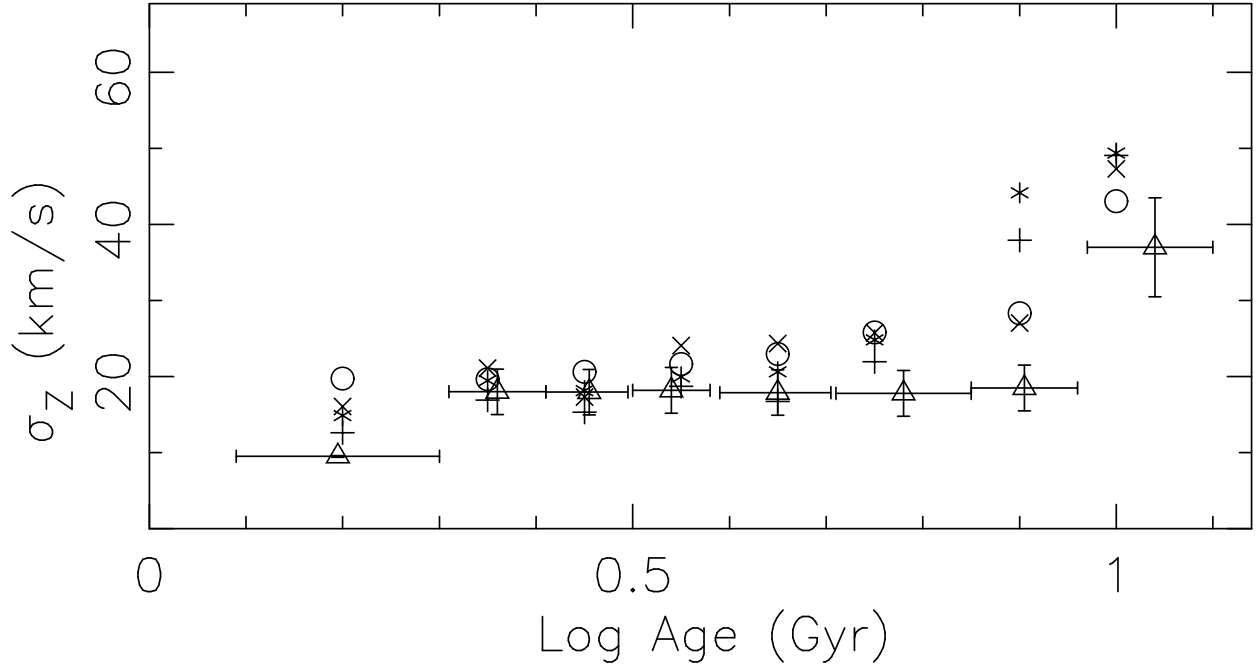


Fig. 2.— Velocity dispersion for the direction of perpendicular to the plane (Z direction) as a function of the age for four sGALS: sGAL1/2/3/4 is designated by symbols +/*/o/x, respectively. The velocity dispersion is measured around star particles within $6 < R_{XY} < 10$ kpc and $|Z| < 1$ kpc. Also shown by triangles with error bars are observations of solar neighborhood stars, as derived by Quillen & Garnett (2001, Fig. 3) from the sample of Edvardsson et al. (1993). In each of our sGALS, as well as the observations, an abrupt increase in the velocity-dispersion is apparent at lookback times > 8 Gyr. This abrupt increase is a signature of the thick disk. sGAL1 and sGAL2 show an abrupt increase at lookback time ~ 8 Gyr, while the upturn in velocity dispersion in sGAL3 and sGAL4 is at an earlier time, closer to the lookback time of ~ 10 Gyr observed for the Milky Way.

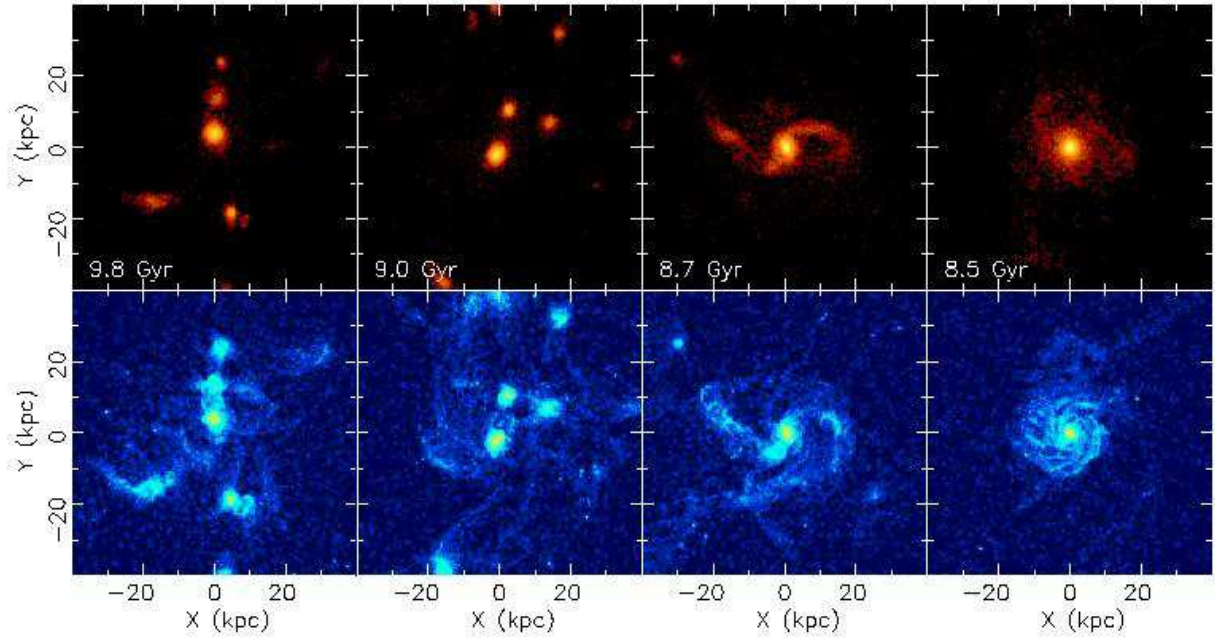


Fig. 3.— Density plots of stars (upper panels) and gas (lower panels) of sGAL1 during the epoch of thick disk formation, shown face on (X-Y plane). Four time-steps are shown, at lookback times ranging from 9.8-8.5 Gyrs. This epoch corresponds to the time at which the velocity dispersion-age relation shows a sharp increase, indicating the presence of a thick disk (Fig. 2), and is characterized by gas rich merger events. At the beginning of this sequence, several gas rich galactic "building blocks" exist, while at the end of this epoch, a central sGAL has formed.

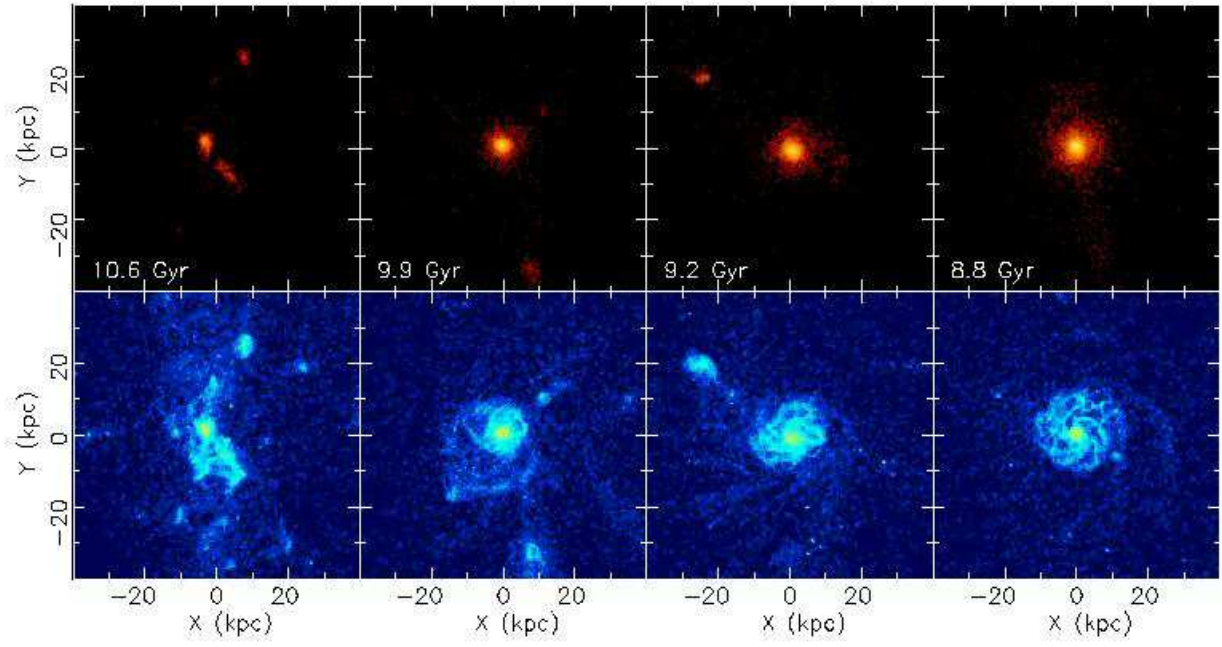


Fig. 4.— Same as in Figure 3, but for sGAL2.

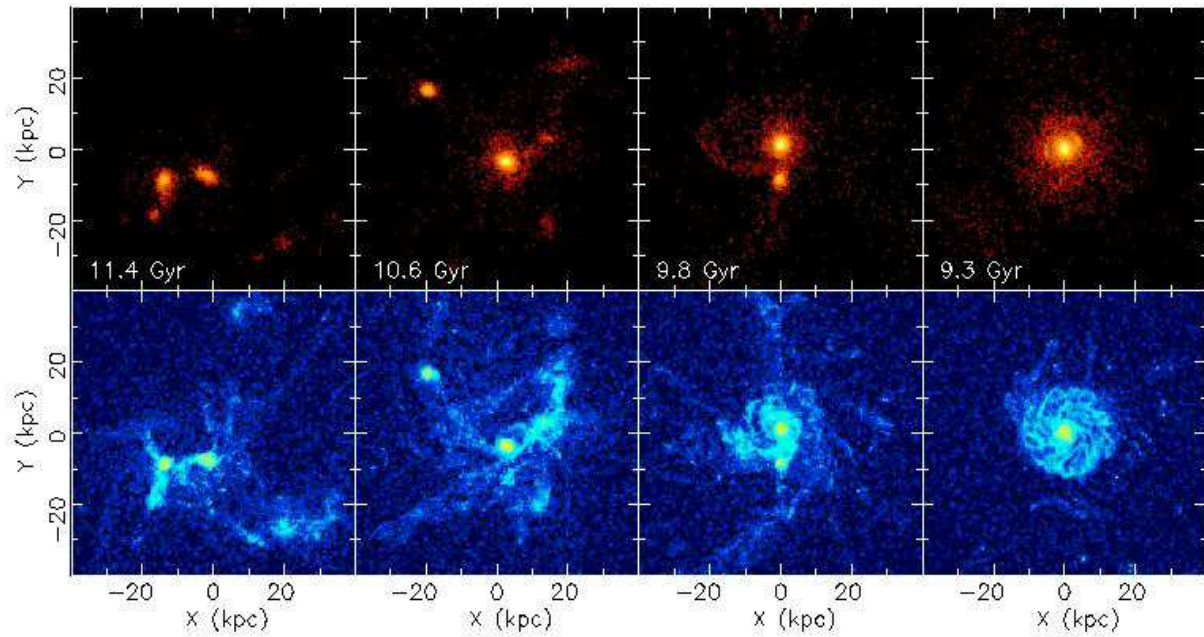


Fig. 5.— Same as in Figure 3, but for sGAL3. We see that the epoch of gas rich mergers which we associate with thick disk formation is earlier in this sGAL than in sGAL1 and sGAL2, consistent with the older lookback time of the abrupt increase in velocity dispersion seen in Figure 2, as well as the time of the peak of the star formation rates (Fig. 7).

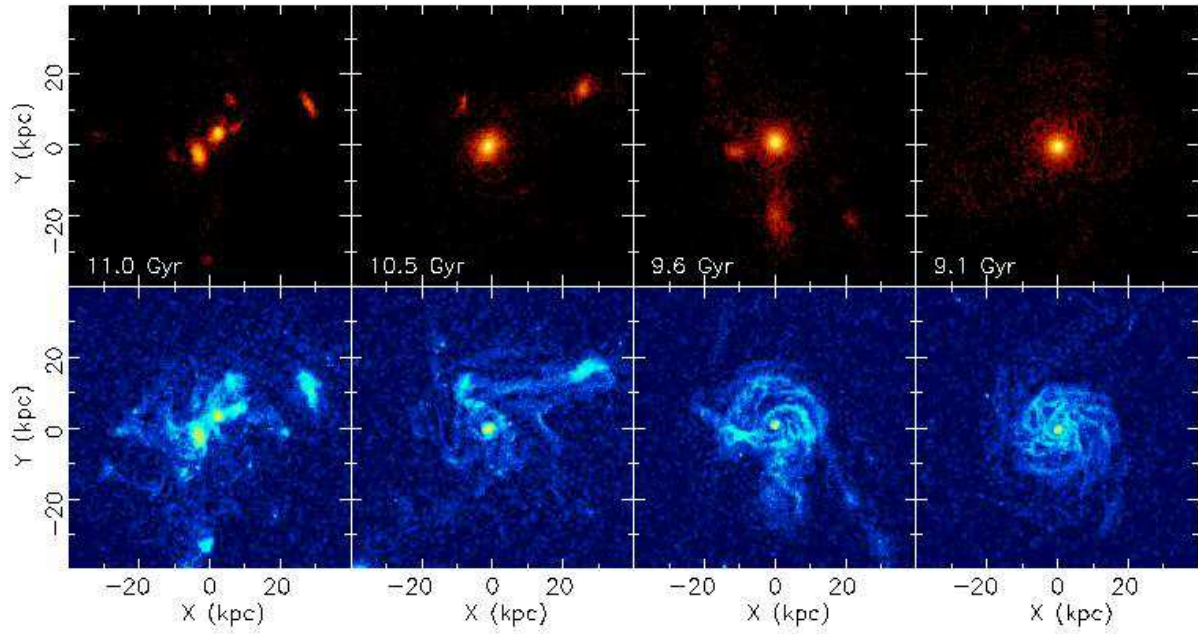


Fig. 6.— Same as in Figure 3, but for sGAL4.

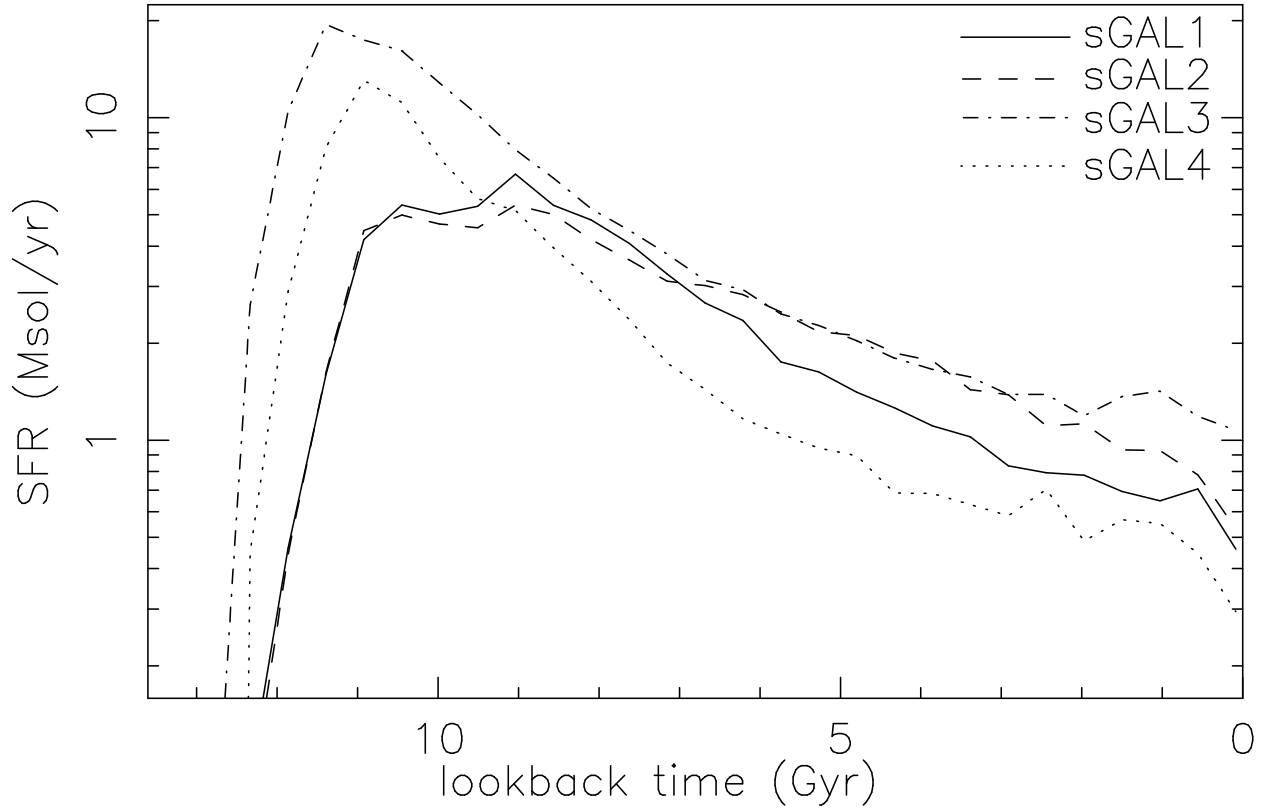


Fig. 7.— Global star formation rate (SFR) as a function of lookback time for sGALS. The solid, dashed, dot-dashed, and dotted lines indicate the SFR of sGAL1, sGAL2, sGAL3, and sGAL4, respectively. The peaks of the SFR correspond to the epochs of gas rich merging which we associate with thick disk formation period. Note that sGAL1 and sGAL2 have the peaks of the SFR at later a epoch than sGAL3 and sGAL4, corresponding to the later occurrence of the gas rich merging epoch in these sGALS, as shown in Figures. 3-6.

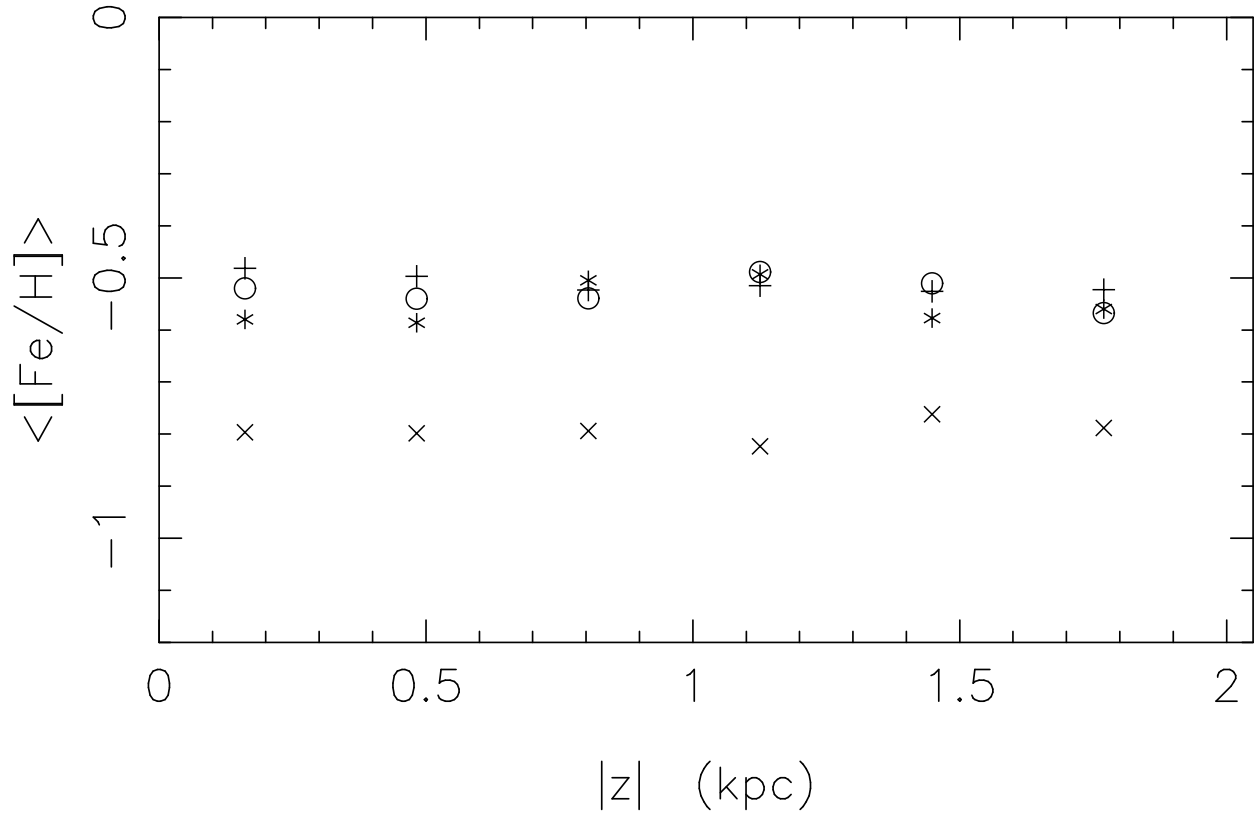


Fig. 8.— Mean iron abundance ($\langle [\text{Fe}/\text{H}] \rangle$) as a function of the distance from the disk plane, i.e. height ($|z|$) for thick disk stars. The same symbols as Figure 2 are used. Thick disk stars of sGAL1, sGAL2 and sGAL3 have $\langle [\text{Fe}/\text{H}] \rangle$ between -0.5 and -0.6 , while thick disk stars in sGAL4 have a lower metallicity, $\langle [\text{Fe}/\text{H}] \rangle \sim -0.8$. Very little gradient is apparent for the thick disk star particles of all four sGALS.

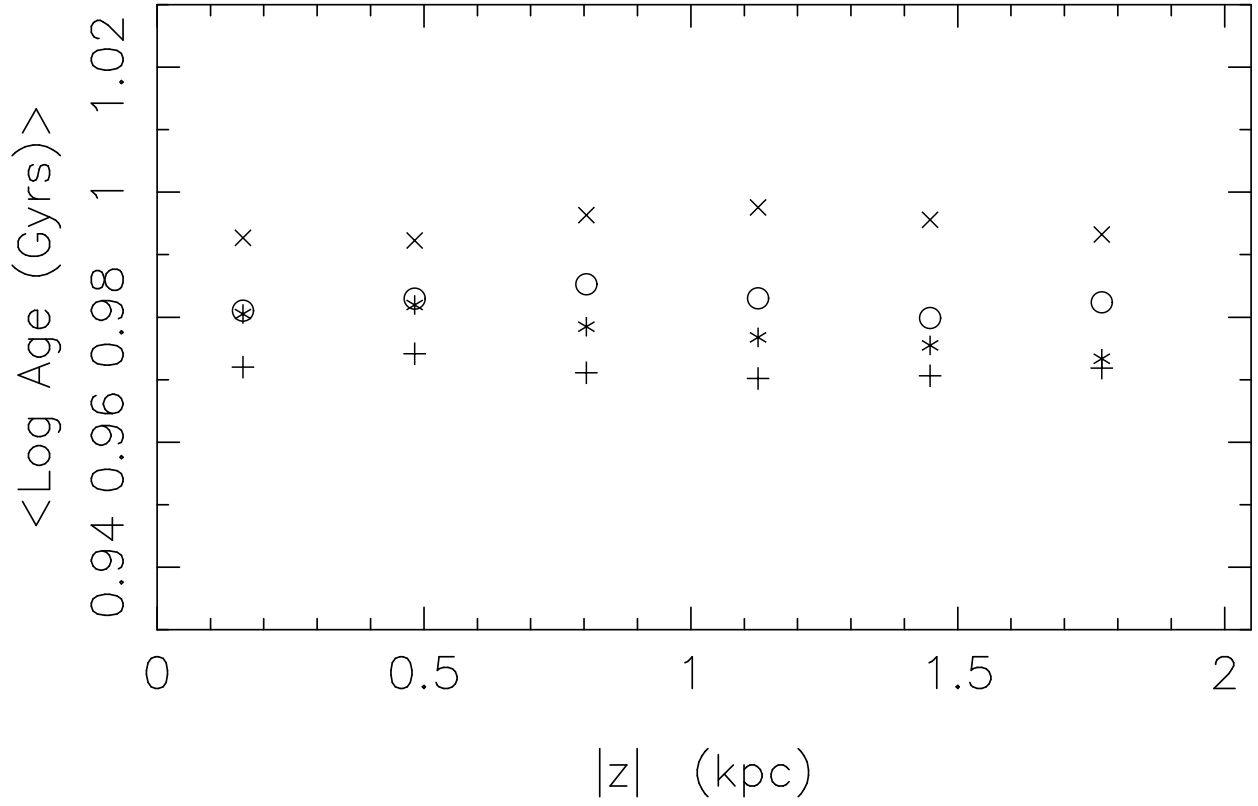


Fig. 9.— Mean of logarithm of age (Gyrs) as a function of $|Z|$ for thick disk stars. The same symbols as Figure 2 are adopted. Thick disk stars in each galaxy are old, with little or no variation with height.

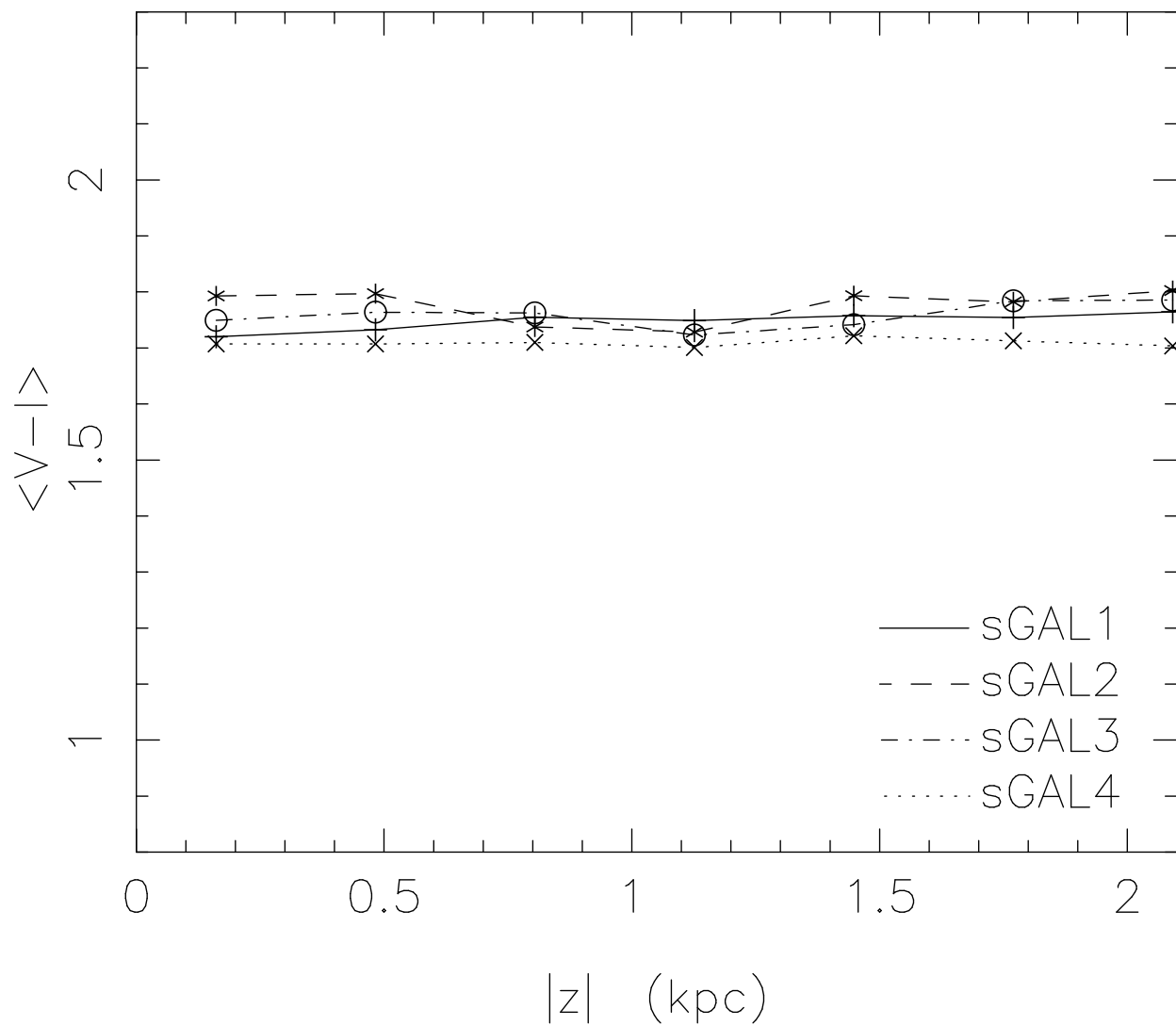


Fig. 10.— Mean $V - I$ color as a function of $|Z|$ for the giant branch stars (RGB/AGB) of the thick disk stars in sGALS. The same symbols as Figure 2 are employed.

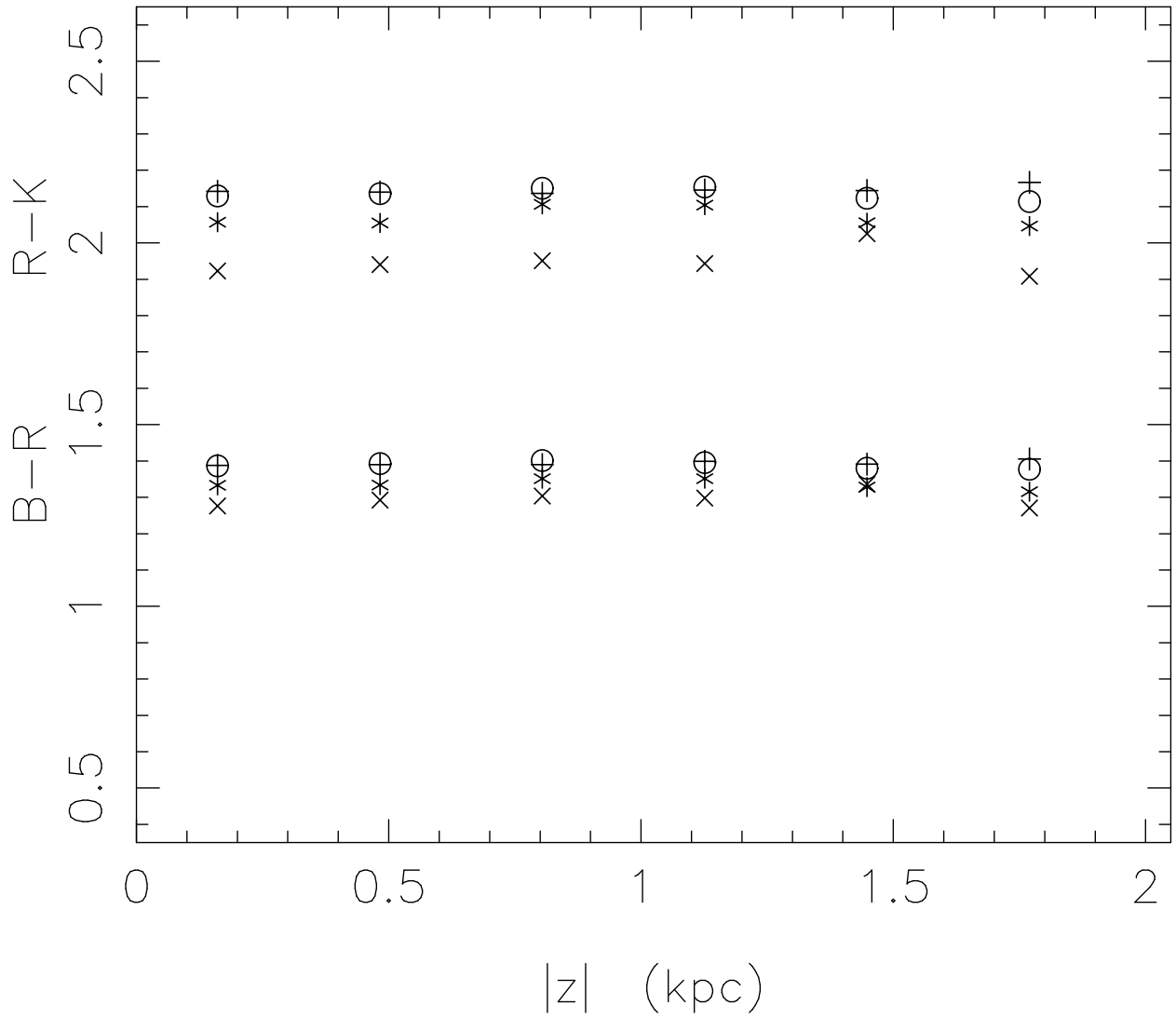


Fig. 11.— Mean $B-R$ and $R-K$ colors as a function of $|Z|$ for the thick disk stars of sGALS. Symbols used in Figure 2 are employed.

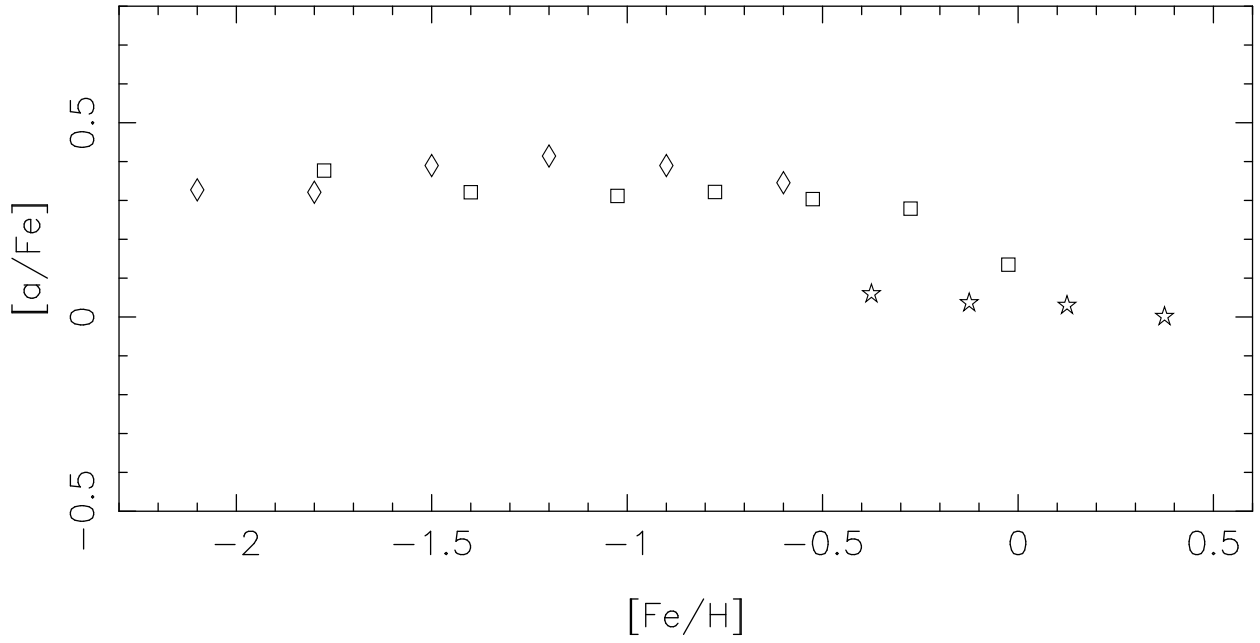


Fig. 12.— $[\alpha/\text{Fe}]$ versus $[\text{Fe}/\text{H}]$ for solar neighborhood stars of sGAL1. Thin disk, thick disk, and halo stars are represented by star, square, and diamond symbols, respectively.

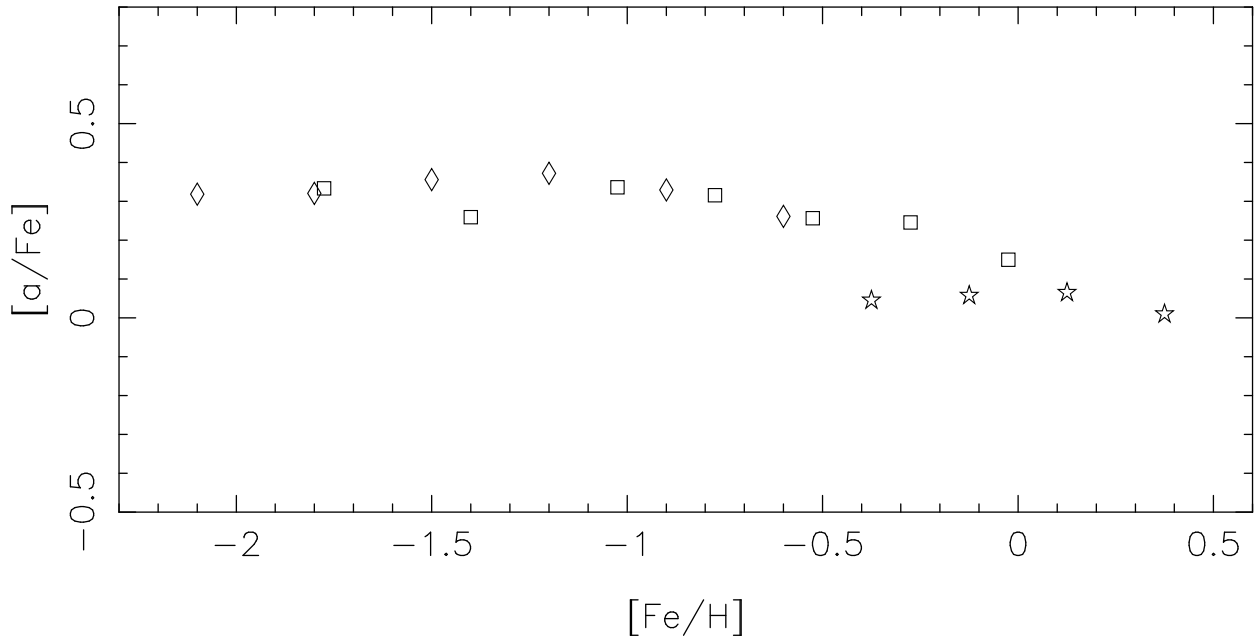


Fig. 13.— Same as Figure 12, but for sGAL2.

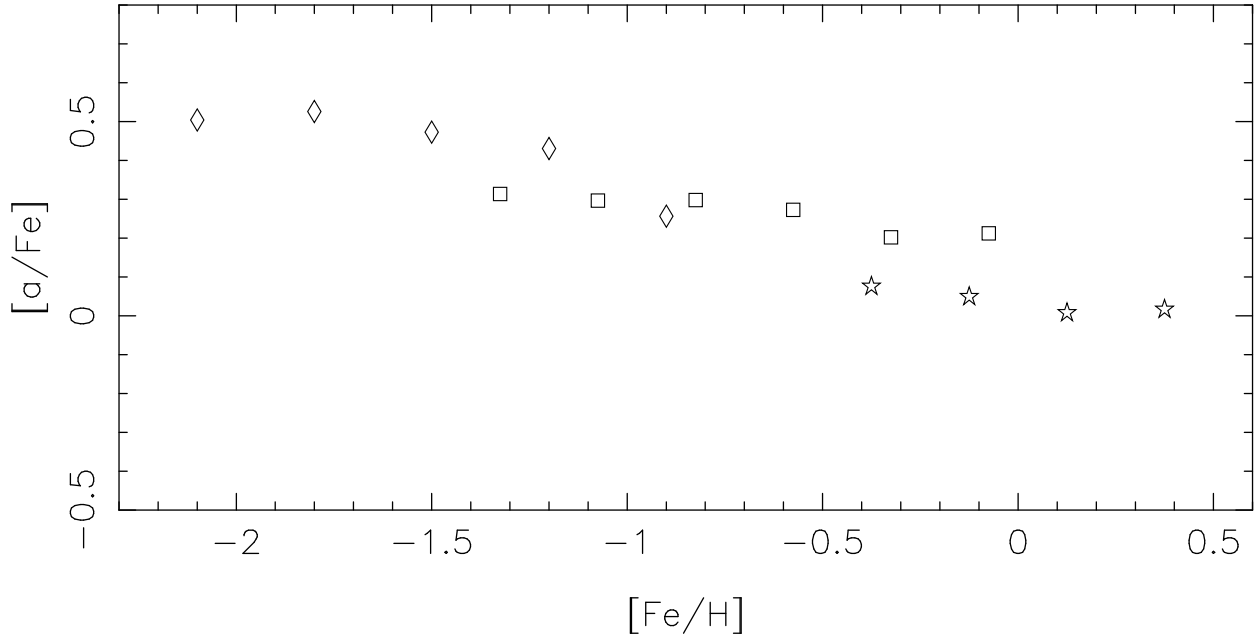


Fig. 14.— Same as for Figure 12, but for sGAL3.

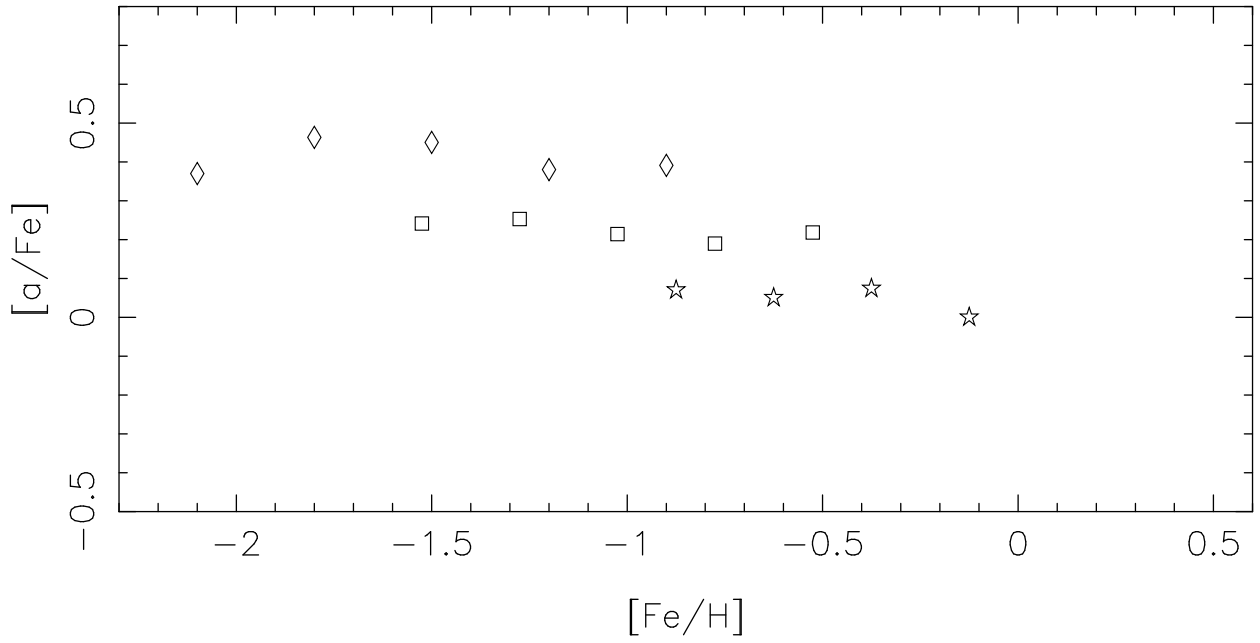


Fig. 15.— Same as for Figure 12, but for sGAL4.

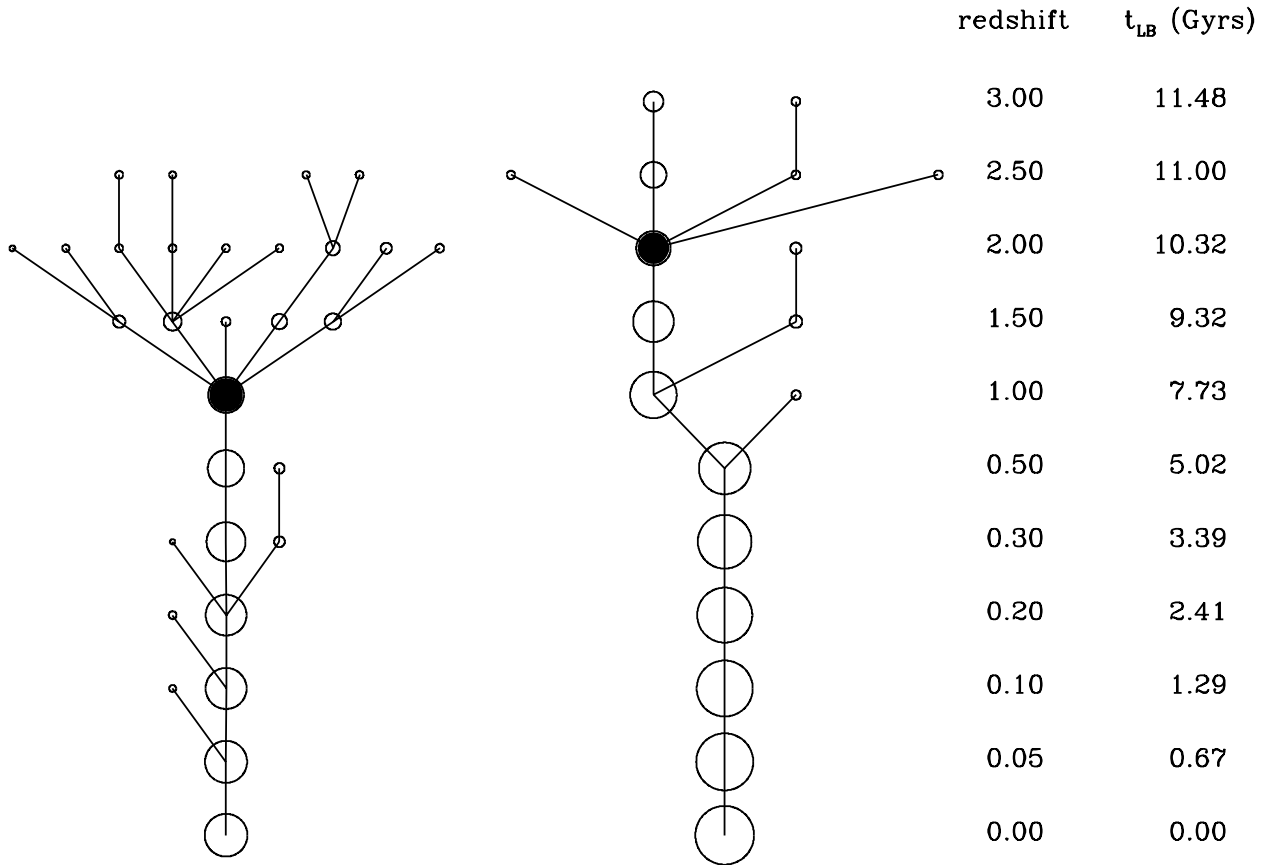


Fig. 16.— Merger trees for two of our 58 simulated halos that are Milky Way analogs. The tree on the left (right) is referred to as halo 1 (2) in the text. Within each tree, the area of each circle is proportional to the mass of the halo, and the black circle identifies the product of the greatest merger epoch. Redshifts and lookback times are indicated on the right side.

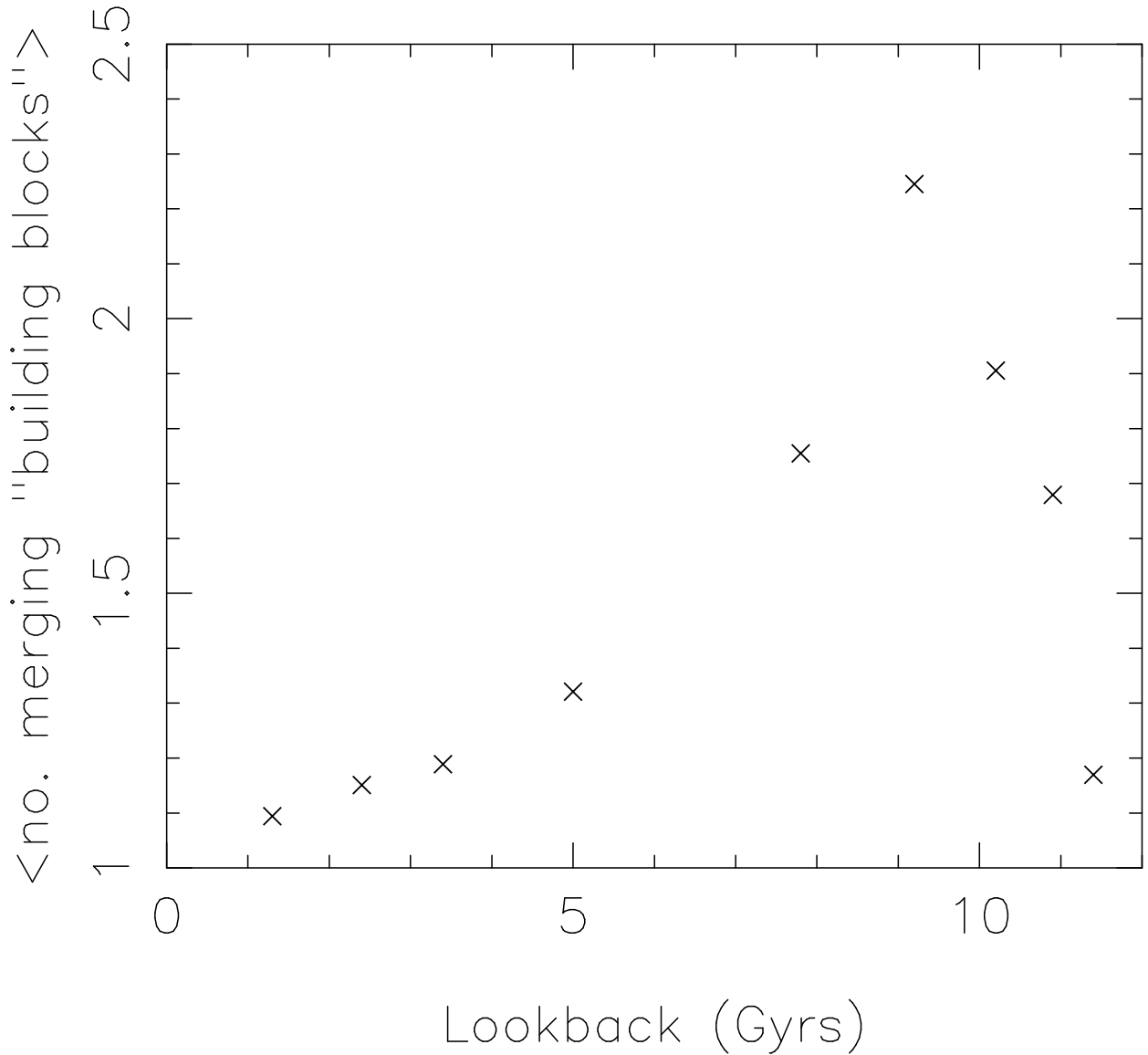


Fig. 17.— Average number of “building blocks” versus lookback time for our 58 Milky Way sized dark matter halos. In order to qualify, the “building block” must be $\geq 10^{10}M_{\odot}$, add at least 4% to the mass of the halo, and be merged to the largest (central) halo by the next timestep. Thus, this plot summarizes the history of “significant merging” in the build up of Milky Way sized halos.